Deliverable D 3.9
Models of the industrial structure

Document type	**Deliverable D 3.9**
Document Version / Status	**1.2**
Primary Authors	**Alain GASSER, alain.gasser@univ-orleans.fr, UORL**
Distribution Level	**PU (Public)**
Project Acronym	**ATHOR**
Project Title	**Advanced THermomechanical multiscale mOdelling of Refractory linings**
Grant Agreement Number	**764987**
Project Website	www.etn-athor.eu
Project Coordinator	**Marc Huger, marc.huger@unilim.fr, UNILIM**
Document Contributors	**Eric BLOND, eric.blond@univ-orleans.fr, UORL** **Alain GASSER, alain.gasser@univ-orleans.fr, UORL** **Mahmoud ALI, mahmoud.ali@univ-orleans.fr, UORL** **Soheil SAMADI, soheil.samadi@unileoben.ac.at, MUL**

History of Changes

Version	Date	Author (Organization)	Change	Page
1.0	13/03/2022	Soheil Samadi (MUL)	First draft	all
1.1	28/03/2022	Mahmoud ALI (UORL)	Modelling using homogenization approach	all
1.2	29/03/2022	Glyn DERRICK (UNILIM) Marc HUGER (UNILIM)	Final Check	all

TABLE OF CONTENTS

1 Introduction

In this deliverable, a simplified industrial scale steel ladle has been simulated using two modelling approaches developed within the framework of ATHOR project. The first modelling approach is the unit cell approach developed at MUL and the second approach is the homogenization approach developed at UORL. Details about the two approaches, physical models, simulation techniques, thermal and mechanical boundary conditions are reported in this deliverable. Transient thermomechanical analysis of a steel ladle were performed using two approaches. The impacts of the creep and stress relaxation, caused by the viscoplastic behaviour of refractories at high temperature, on the thermomechanical behaviour of the ladle are shown and explained. The results and discussion of the thermal and thermomechanical fields during five thermal cycles of the ladle are reported.

2 Steel ladle description

The objective of the current study was thermomechanical simulation of a steel ladle refractory lining. The 2D drawing of the steel ladle with its refractory linings is shown in Figure 1.

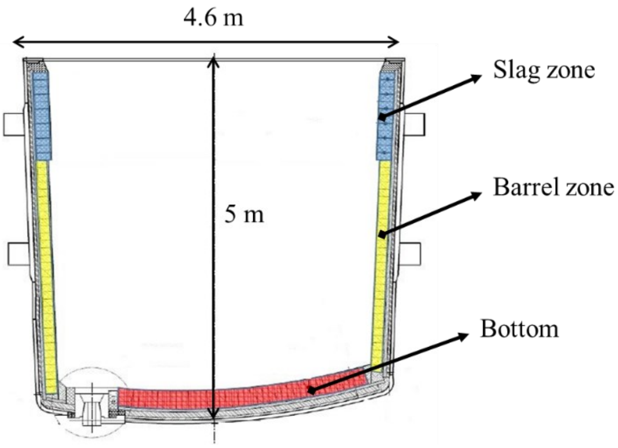

Figure 1: 2D Sketch of the industrial steel ladle.

Table 1 lists the refractory materials used in each section of the ladle. In addition to the refractories indicated, shotcrete and insulating board were utilized in the construction of the ladle lining.

Table 1: Refractory materials used in the steel ladle.

Section	Material	Masonry type
Working lining Barrel zone	Alumina spinel bricks	With dry joints
Working lining Slag zone	Magnesia carbon bricks	With dry joints
Working lining bottom	Alumina magnesia carbon bricks	With dry joints
Safety lining	Bauxite bricks	With mortar joints
Insulation lining	Chamotte bricks	With mortar joints

The definition of a steel ladle working cycle depends on its purpose. The steel ladle studied in this deliverable was employed in a working cycle plan according to Table 2.

Table 2: Working cycles of the studied steel ladle.

Title	Duration	Temperature
Preheating	1 hour	25 °C - 600 °C
	13 hours	600 °C - 1050 °C
	2 hours	1050 °C
Pouring	7 minutes	1050 °C - 1650 °C
Processing	125 minutes	1650 °C
Casting	45 minutes	1650 °C
Idle time	2 hours	Adiabatic condition

3 Modelling using a representative volume element

The unit-cell modelling technique employs a representative volume element that contains all constitutive data, such as all units and joints, and is a repeatable piece of the lining. Simulating a representative volume element instead of the complete structure results in a smaller model size and therefore lower computational cost [1]. Nevertheless, it requires the knowledge of each part of the refractory lining. This knowledge can be gained through experiments on meso-scale specimens.

Here, a 3D representative volume element model of the steel ladle (shown in Figure 2) was built using the commercial software Abaqus [2] according to its industrial design and dimensions. The model has a cone shape and because of the existing symmetry conditions, its thickness was considered as half of an alumina spinel brick, which is used in the working lining barrel zone.

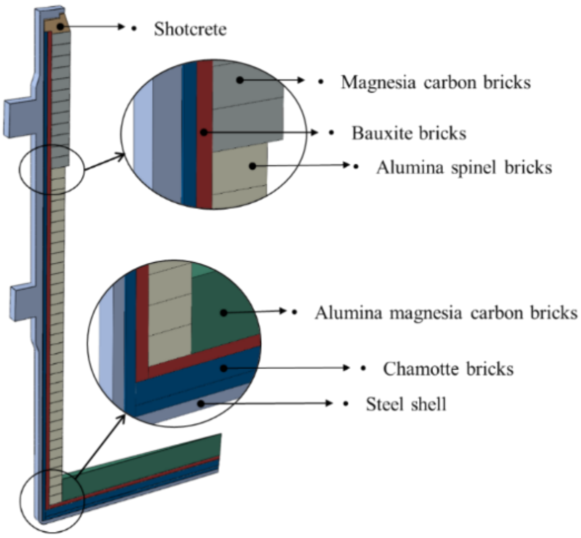

Figure 2: 3D unit-cell model of the steel ladle refractory lining.

Regarding the boundary conditions in the model, firstly, the symmetry plane of the bricks and the bottom of the steel shell were constrained from moving in the perpendicular directions of their surface. In addition, to consider the effect of the joints between the bricks in the working lining, the following measures were considered in the model (as shown in Figure 3). A rigid plate is used to consider the vertical joints (head joints), which was defined 0.4 mm. In addition, to account for the effect of the horizontal joints between the bricks (bed joints), initial 1 cm gap between the shotcrete and shell was defined. Another model simplification was about the thermal effect of the insulation board. The 5 mm thick insulating board between the chamotte bricks and the steel shell has a low rigidity and hence has little impact on the stress distribution. Instead of simulating this part, the contact between the chamotte bricks and the steel shell was described using the insulation board's conductivity of 0.06 J/smK. The effect on the model's heat distribution is thus considered without adding to the model's complexity. Finally, the mechanical contact definition between the parts was frictionless.

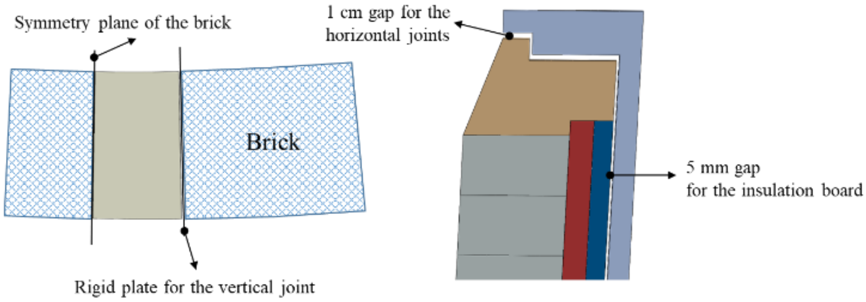

Figure 3: Consideration of joints in the steel ladle unit-cell model.

In this study, the goal was to compare the elastic and creep behaviour of the refractory lining. Therefore, two simulations, one using the isotropic elasticity model, and one using the Norton-Bailey creep model in Abaqus were performed. The material properties necessary for these thermomechanical simulations are indicated in Table 3. Physical and thermal properties were required for all parts of the model, however the creep properties were assigned only to the working lining.

Table 3: Material properties required for the thermomechanical simulations.

Physical properties	Thermal properties	Creep properties
Young's modulus	Coefficient of thermal expansion	Norton-Bailey parameters
Poisson's ratio	Conductivity	A, n and m
Density	Specific heat	-

The material properties of the alumina spinel bricks are reported in Table 4 and 5.

Table 4: Alumina spinel bricks material properties used in thermomechanical simulation.

Material properties		Value						
Physical	***Temperature (°C)***	25	250	500	750	1000	1250	1500
	Young's modulus (GPa)	35.1	34.7	33.9	34.5	37.5	37.5	38.0
	Poisson's ratio (-)	0.2						
	Density (kg/m³)	3130						
Thermal [3]	***Temperature (°C)***	25	200	400	800	1000	1200	1500
	Conductivity (J/smK)	6.42	4.85	3.79	2.94	2.66	2.41	
	Specific heat (J/kgK)	805	1073	1161	1263	1293	1318	
	CET (10^{-6}/K)	5.40	7.08	7.56	8.23	8.47	8.66	8.65

Table 5: Creep parameters of alumina spinel at different temperatures.

	Temperature (°C)	**900**	**1300**	**1400**	**1500**
Creep [4]	**A (Pa^{-n}/s)**	$1e^{-26}$	$7.75e^{-12}$	$1.72e^{-14}$	$2.18e^{-08}$
	n	0.0001	1.1387	1.5905	0.6749
	m	-0.5	-0.7322	-0.7257	-0.6631

4 Modelling using the homogenization approach

In the homogenization technique, the bricks and joints are replaced by a continuous homogeneous medium whose effective mechanical properties depend on the state of bed and head joints (open or closed). The developed 3D solution domain of the steel ladle is shown in Figure 4. Only one quarter of the ladle was modelled to reduce the computational size of the problem. This approach is valid since the studied ladle is symmetric. The working lining (bottom and wall, masonry with dry joints) was replaced by a homogeneous medium and the developed multi scale constitutive material model of masonry with dry joints was used to describe the mechanical behaviour of the working linings (layer in contact with liquid steel). Further details about the development, validation and implementation of this constitutive material model are given in deliverables 3.6 and 3.7. Details about the material of each layer are given in Figure 2. The thermophysical and mechanical properties of all linings are similar to those given in section 3.

Regarding the boundary conditions of the model, symmetry boundary conditions have been applied to the symmetric planes of the physical model of the ladle. The outer surface of the steel shell's bottom was assumed to be fixed in the vertical direction. The weight and hydro-static pressure of the liquid steel were neglected as their impacts on resulting stresses are very small (around 1 MPa) as compared to the impact of the thermal expansion of the bricks (around 100 MPa in some cases). The frictional interactions between the different layers of the ladle are considered in the numerical model using surface to surface contact in Abaqus (coefficient of friction 0.5).

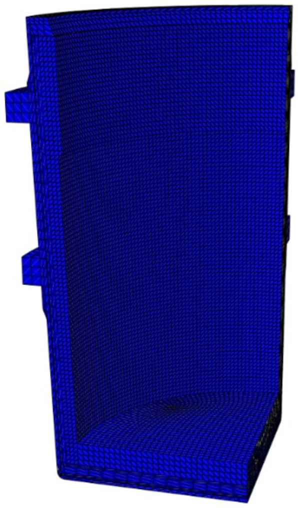

Figure 4: 3D solution domain and mesh of the steel ladle used in the homogenization technique.

5 Results and comparisons

Firstly, the results of the thermomechanical simulations using 3D unit-cell and homogenization models are presented. In total, five steel ladle process cycles were simulated. The temperature results are shown in Figure 5. The temperature on the steel shell increased to around 290 °C at the end of fifth idle time; nevertheless, the temperature increase rate slowed down with time. The insulation layer cold-face temperature was around 900 °C at the end of fifth idle time, which proved the importance of the insulation board located between the insulation bricks and the steel shell. Moreover, the temperature of the lining was increasing constantly due to the fact that the adiabatic condition was considered for the hot face of the bricks, which is only the case if the lid of the ladle is not removed during the idle time. The differences between the two modelling approaches are caused by the physical representation of the insulation layer in the model. In the representative volume element modelling approach, the 5 mm thickness insulating board between the chamotte bricks and the steel shell has been considered by modifying the thermal conductance in the thermal contact (0.06 J/smK) between the chamotte bricks and the steel shell. On the other hand, in the homogenization approach, the insulation board was physically represented and the corresponding thermophysical properties were used.

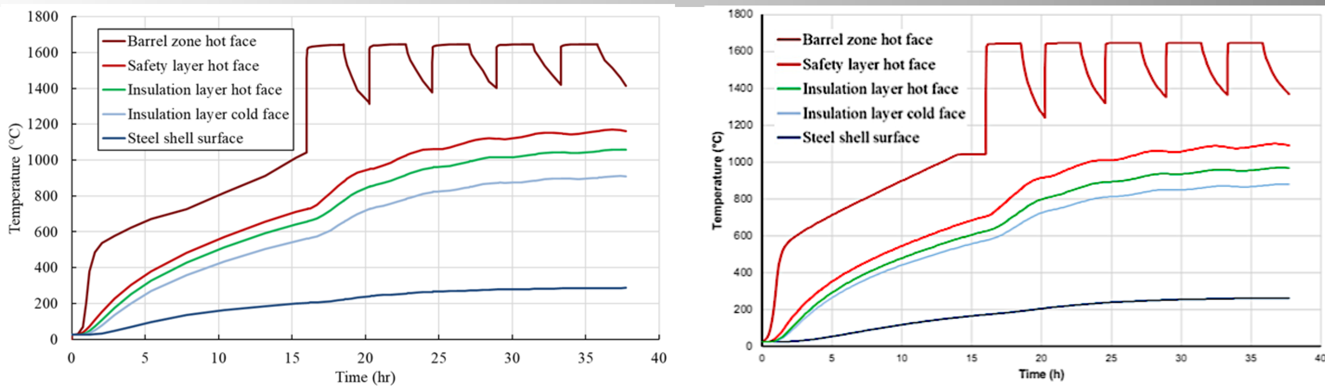

(a) (b)

Figure 5: Simulated temperature of different layers in barrel zone (preheating and five working cycles): (a) representative volume element approach and (b) homogenization approach.

In the whole working lining, it was observed that the maximum von Mises stress occurred for the elastic simulation and the least von Mises stress occurred for the creep model due to the relaxation. Moreover, for better comparison of the simulations, one brick from the middle of barrel zone was chosen (Figure 6).

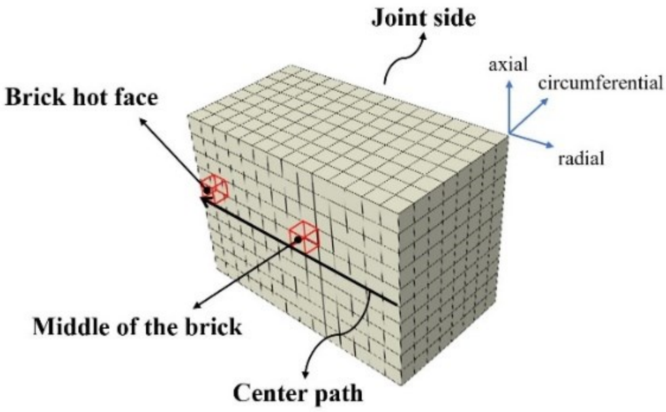

Figure 6: Alumina spinel brick model

In Figure 7, radial, circumferential, and axial stresses at the hot face and the middle of the selected alumina spinel brick were shown during all process time. The stresses are the mean values of 8 integration points in the element. The first observation was that a biaxial compressive stress state existed in the centre of brick, i.e., radial stress was negligible compared to axial and circumferential stress. The stress magnitudes during the preheating are around the same magnitude for elastic and creep models. In addition, the creep decreased the stress on the hot face in the beginning of 1st cycle, and in the middle of the brick, during the 2nd cycle. The creep occurred after the temperature increased sufficiently and it started in the middle of the brick with a delay from the hot face. Therefore, the equivalent creep strain was higher on the hot face than the other parts of the brick. The differences between the resulting thermomechanical stresses obtained by both modelling approaches are caused by the major difference between the solution domains of both approaches and the related boundary conditions applied to the sides of the ladle (rigid plate in the RVE approach and symmetry in the homogenization approach). The comparison between the micro and macro modelling approaches could be more useful if the solution domains and physical representations of the problem of both approaches are the same.

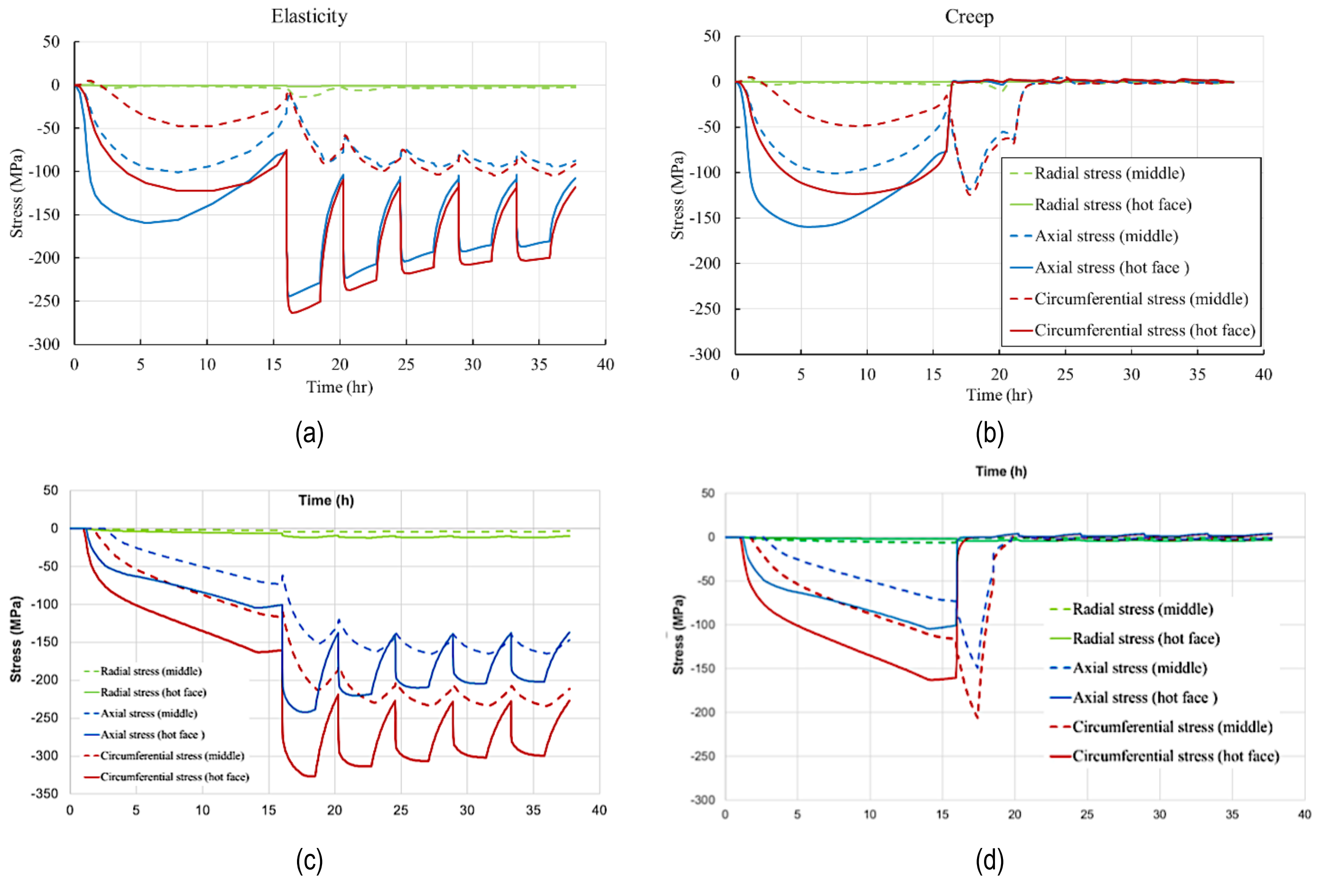

Figure 7: Stress at the hot face and middle of the selected alumina spinel brick: (a and b) representative element approach, (c and d) homogenization approach.

The horizontal joint openings were negligible compared to the vertical ones, and they occurred mostly for the cold side of bricks (less than 0.1mm). It was observed that at the end of 5th cycle, for the creep simulation there was joint opening for all working lining bricks at the hot face, while the elastic simulation did not show opening at this time point. Figure 8 shows the vertical joint opening at the hot face of the selected alumina spinel brick during the time.

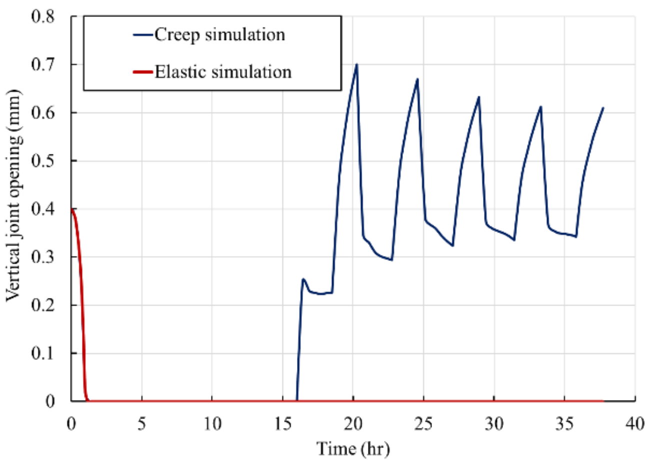

Figure 8: Vertical joint opening on the alumina spinel brick hot face

In Figure 9, the von Mises stress from both simulations at the end of fifth cycle was compared. The view shows the centre, back and top of the brick. It was observed that the maximum von Mises stress occurred for the elastic simulation. The lowest value of the von Mises stress occurred for the creep model due to the relaxation, and it was observed that maximum stresses were on the cold face of the brick on which creep has not affected yet.

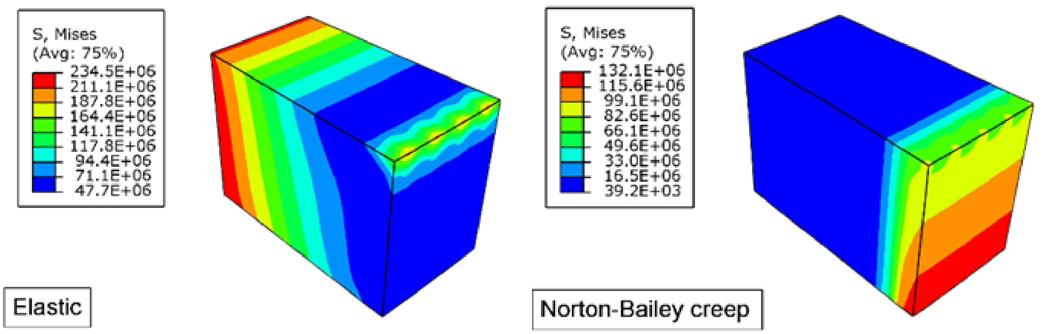

Figure 9: Mises stress in an alumina spinel brick from the middle part of the barrel zone at the end of 5th idle time.

In Figure 10, the equivalent irreversible creep strain is shown. The view is the alumina spinel brick cut horizontally in the middle. The creep strain was higher near the joint than in the centre of the brick.

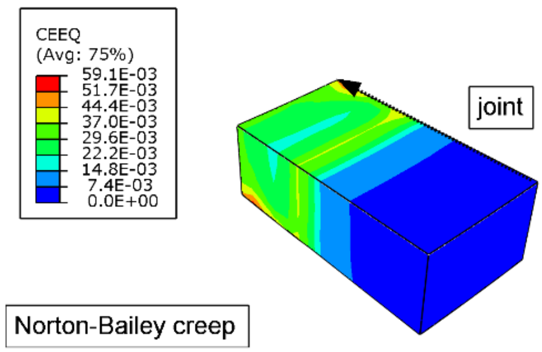

Figure 10: Equivalent creep strain in an alumina spinel brick from the middle part of the barrel zone at the end of 5th process cycle.

6 Conclusion

In the present work, transient thermomechanical analysis of a simplified steel ladle were carried out. The analysis have been performed using two modelling approaches developed at MUL and UORL namely: representative volume element approach and homogenization approach. First, transient heat transfer analysis were carried out to determine the temperature variations of the linings with time. These fields, in turn, have been used as thermal fields for the transient thermomechanical analysis. In the representative volume element approach, the bricks and the joints are considered separately. On the other hand, and in the case of the homogenization approach, the bricks and joints are replaced by a homogeneous material model whose mechanical properties depends on the state of bed and head joints (closed or open). The impacts of the mechanical constitutive behaviour laws on the resulting thermomechanical stresses were studied. Generally, it has been showed that the creep caused joint opening and reduced the stresses in the working lining for both the unit-cell and homogenization modelling approaches. However, the time variations of stresses in the working lining predicted by the two modelling approaches were different. The difference was mainly caused by the major difference between the physical representation of the solution domain of the ladle. This led to different boundary conditions applied to the sides of the ladle.

It has been observed that the working lining was subjected to multiaxial stress state. The application of uniaxial creep parameter might lead to overestimation of the creep strains and joint openings when creep is considered because the refractories might show different creep behaviour under multiaxial stresses. Further parametric studies to investigate the impacts of joints thickness, joints behaviour, constitutive material models of each layer and material properties on the thermomechanical performance of the ladle are given in deliverable 3.10.

7 References

[1] K. Andreev, H. Harmuth, FEM simulation of the thermo-mechanical behaviour and failure of refractories—a case study, Journal of Materials Processing Technology. 143–144 (2003) 72–77. https://doi.org/10.1016/S0924-0136(03)00322-4.

[2] Dassault systems, ABAQUS (2018) 'ABAQUS Documentation,' (2018).

[3] D. Vitiello, Thermo-physical properties of insulating refractory materials, Ph.D. thesis at University of Limoges, 2021.

[4] S. Samadi, S. Jin, D. Gruber, H. Harmuth, Creep parameter determination of a shaped alumina spinel refractory using statistical analysis, in: Proceedings of 63rd International Colloquium on Refractories, Raw Materials and Reuse, 2020: pp. 1–5.

European Commission
Horizon 2020
European Union funding
for Research & Innovation